



Simple and rapid preparation of CuO film using SILAR process for application as hole-transporting layer in p-i-n perovskite solar cell

Sutthipoj WONGRERKDEE^{1,*}, Kritsada HONGSITH^{2,3}, Supab CHOOPUN^{2,3,4}, Khathawut LOHAWET⁵, and Pisist KUMNORKAEW⁵

¹Department of Physics, Faculty of Liberal Arts and Science, Kasetsart University Kamphaeng Saen Campus, Nakhon Pathom 73140, Thailand

²Department of Physics and Materials Science, Faculty of Science, Chiang Mai University, Chiang Mai 50200, Thailand

³Thailand Center of Excellence in Physics (ThEP center), CHE, Bangkok 10400, Thailand

⁴Center of Advanced Materials for Printed Electronics and Sensors, Faculty of Science, Chiang Mai University, Chiang Mai, 50200, Thailand

⁵National Nanotechnology Center, National Science and Technology Development Agency, Pathum Thani, 12120, Thailand

*Corresponding author e-mail: sutthipoj.s@ku.ac.th

Received date:

12 May 2018

Accepted date:

17 June 2018

Keywords:

Copper oxide
SILAR process
Hole-transporting layer
Perovskite solar cell

Abstract

Copper oxide (CuO) films are considered to be an alternative metal oxide semiconductor for hole-transporting layer application in p-i-n perovskite solar cells due to their unique properties including intrinsic p-type materials and energy band level matching. The films can be synthesized using several methods such as sputtering, solution process and spin-coating processes. However, using the successive ionic layer adsorption and reaction (SILAR) process to prepare a CuO hole-transporting layer in p-i-n perovskite solar cells is still underreported. Thus, this study prepared the SILAR processed CuO films and applied as a hole-transporting layer in p-i-n perovskite solar cells. The results showed that morphology of CuO films is slightly changed when the SILAR cycles is increased, in correlation to the increasing of detected copper element. High optical transmittance in visible light region is found for all conditions, indicating a good transparent film for optoelectronic device likely to solar cells. For solar cell application, a commercial PEDOT:PSS hole-transporting layer was used in a p-i-n perovskite solar cell and compared with the CuO films. The solar cells fabricated with CuO films produced lower performance than that fabricated with commercial PEDOT:PSS. The low performance resulted from the incomplete formation of perovskite films when they are deposited onto CuO films, causing carrier loss due to the recombination effect. However, power conversion efficiency was observed where the solar cell was fabricated with CuO films, which could be attributed to the potential of CuO films as an alternative hole-transporting layer in p-i-n perovskite solar cells. The study indicated that the SILAR method could be an alternative offering a simple, fast, and low cost process for p-i-n perovskite solar cell application.

1. Introduction

Perovskite solar cells (PSCs) are the most popular emerging solar cell in research and commerce due to their unique properties. PSCs not only reach a high power conversion efficiency (PCE) in short research durations or in large scale fabrication, but also have re-productivity [1-6]. This advantage is a challenge for commercial and sustainable consumption. The original structure of PSCs was well-presented as n-i-p PSCs including mesoscopic and planar structures [7-10] which were fabricated as a sequential deposition layer by layer of an n-type semiconductor as an electron transporting layer (ETL), perovskite (PS), and a p-type semiconductor as a hole-transporting layer (HTL), respectively [11]. Popular ETLs such as

TiO₂ and ZnO have limited electron transport in PSCs because they have relative low mobility compared with PSs [8,12]. The effect of low mobility leads to an imbalance of electron-hole transportation and results in the accumulation of charge which can be detected from the hysteresis effect [13]. To solve the problem, high quality films have been used with several techniques such as interface engineering modification [14], additive modification [15-16], heat treatment [17], surface treatment [18-19] and chemical control [20]. These methods resulted in successful, enhanced PCE, however, some unexpected results were found such as unstable PCE, inappropriate required energy, and a relatively high expense. One effective method was developed by inverting the PSC structure from n-i-p to be p-i-n PSCs, and the p-i-n PSCs showed

better carrier transport efficiency than the other form. The p-i-n structure can be demonstrated by sequential deposition step by step of HTL, PS, and ETL, respectively [13,21]. However, most of the excellent HTLs such as PEDOT:PSS, P3HT, and spiro-OMeTAD are expensive [22]. Thus, several intrinsic p-type semiconductors were investigated as alternative HTLs such as NiO, CuSCN [21], CuO_x [23-24], Cu₂O, and CuO [25-26]. Among these, copper oxide groups (CuO_x, Cu₂O, CuO) should be considered as challenging materials because they have not only high hole mobility, but also have energy band level matching with PSs including CH₃NH₃PbI₃, CH₃NH₃PbBr₃, and CH₃NH₃SnI₃ [27]. Moreover, they can be prepared using simple methods such as electrodeposition [28], spin-coating process [23-24], solution process [29], and the successive ionic layer adsorption and reaction (SILAR) method [30-31]. Several reports presented preparations of copper oxide using different methods for p-i-n perovskite solar cell application. For examples, CuO_x films prepared by simple spin-coating process were applied as an HTL in p-i-n PSCs [23-24] resulting in enhanced PSC performance with good stability. The charge carrier separation rate gain increased the short-circuit current density (J_{sc}) due to the unique high work function of CuO_x films. Nevertheless, the internal recombination was reduced to increase the open-circuit voltage (V_{oc}) because the large grain size formation of perovskite films was supported by hydrophobic CuO_x films. Similar to the CuO_x films, Cu₂O films prepared using electrodeposition were demonstrated as an HTL in PSCs [28]. It was found that the Cu₂O films produced homogenous compact films with a large grain size and were pin-hole free. The Cu₂O acted as growing sites for perovskite formation and resulted in PCE enhancement. Guo *et al.* (2017) [26] prepared Cu₂O and CuO films using magnetron sputtering for HTL application in PSCs, and they suggested a low temperature process for PSC fabrication. Yu *et al.* (2016) [32] found that thickness and the properties of Cu₂O films prepared using thermal oxidation were effective factors to enhance PSC performance. Zuo and Dind, (2015) [25] reported a simple spin-coating process of Cu₂O and CuO films for HTL applied as HTLs in PSCs with high external quantum efficiency. A demonstration of Cu₂O film preparation with a very simple SILAR method for PSC application was presented by Chatterjee and Pal (2016) [31]. PSC performance was enhanced because appropriate

band alignment between the interfaces of Cu₂O/CH₃NH₃PbI₃/PCBM was achieved. The alignment is believed to improve the internal charge behavior which was reflected in the reduced series resistance (R_s) and the increased shunt resistance (R_{sh}).

From the literatures, the preparation of Cu₂O films has been successfully reported for p-i-n PSC application due to low preparation temperature requirement. However, the Cu₂O phase might not be stable for long term use in a high temperature environment while the CuO phase produces more stable materials. CuO films, thus, can be a challenging material in PSCs in a brutal environment. Moreover, an application of CuO films prepared by the SILAR method as an HTL in PSCs has been underreported. This is the first study applying SILAR processed CuO films as an HTL in p-i-n PSC. The films were prepared with different SILAR processed cycles, and characterized using various techniques. After each film was obtained, it was used as an HTL for p-i-n PSC application. The PSC performance was carried out under standard conditions. The results revealed a successful demonstration of the SILAR processed CuO films for application as an HTL in p-i-n PSC.

2. Materials and methods

2.1 Copper oxide film preparation

Before preparing CuO films, F:SnO₂ (FTO) substrate was patterned using Zn metal and a mixed solution of HCl:deionized (DI) water (1/1, v/v). Then the substrate was moved to an ultrasonic bath and cleaned using detergent, DI water, acetone, and isopropanol, respectively, for 15 min each, and finally dried with flowing N₂. A copper precursor was prepared by dissolving 0.1 M Cu(CO₂CH₃)₂·H₂O into distilled water, adding with NH₄OH solution (25 vol.%) to be complex, and stirring for 1 h at room temperature. The H₂O₂ solution used as an oxidizer was prepared by mixing H₂O₂ solution (1 vol.%) into methanol. CuO films were prepared using a SILAR method [33]. The substrate was vertically dipped into the copper precursor, and held for 30 s to adsorb copper ions. After the adsorption process, the substrate was moved and dipped into methanol to remove aggregate ions for 30 s, and then dried for several seconds. The substrate was then dipped into the H₂O₂ solution to oxidize the adsorbed copper ions for 30 s. After the oxidation process, the substrate was dipped into methanol to remove any excess residual, and dried to complete a precursor

film for one cycle of the SILAR process. For additional cycle preparation, the process was sequentially repeated. Finally, the precursor film was annealed at 450°C for 1 h to form CuO films for using as an HTL in p-i-n PSC [30].

2.2 Perovskite solar cell fabrication

Starting solutions consisting of PbI₂, CH₃NH₃I, and PCBM were separately prepared. The PbI₂ solution was prepared by dissolving 1 M PbI₂ into DMF and stirring at 70°C, and the PbI₂ solution is maintained under stirring condition at 60°C to avoid crystallization. The CH₃NH₃I was prepared by dissolving 50 mg·ml⁻¹ into isopropanol and stirring at room temperature. The PCBM solution was prepared by dissolving 30 mg·ml⁻¹ PCBM into chlorobenzene and stirring at room temperature. For the perovskite solar cell fabrication, the CuO films were transferred into a glove box under a flowing N₂ atmosphere to maintain a low relative humidity below 35%. Organic-inorganic perovskite films, CH₃NH₃PbI₃, were prepared onto the top of CuO films using a two-step spin-coating deposition process according to previous work [34]. Briefly, the CuO films were pre-heated at 70°C for 15 min before the spin-coating process. Then, the PbI₂ solution was spin-coated onto the CuO films at 3000 rpm for 30 s, and immediately heated at 70°C for 15 min to form PbI₂ films (yellow films can be observed). After cooling down to room temperature, the CH₃NH₃I solution was spin-coated onto the PbI₂ films at 2000 rpm for 30 s and then heated at 100°C for 2 h to convert the PbI₂ films to be CH₃NH₃PbI₃ perovskite films. After the CH₃NH₃PbI₃ films cooled down to room temperature, the PCBM solution was spin-coated onto the CH₃NH₃PbI₃ films to be ETL. Finally, an Ag electrode was deposited onto the PCBM films using thermal evaporation.

2.3 Characterization

Field emission scanning electron microscopy (FE-SEM, JEOL JSM-6335F), operating at a voltage of 15.0 kV, was used to observe morphology. Energy X-ray dispersive spectroscopy was used to detect chemical elements. Ultraviolet-visible-near infrared (UV-Vis-NIR) spectroscopy was used to investigate optical transmission. Atomic force microscopy (AFM) was used to analyze topology, surface roughness, and thickness. Current density-voltage was measured with a photo

mask active area of 0.04 cm² to evaluate photovoltaic performance, under standard solar illumination of 100 mW/cm² (AM1.5). Open-circuit voltage decay (OCVD) was performed to determine charge dynamics.

3. Results

Morphology of the copper oxide film prepared on FTO substrates using the SILAR process for different cycles of 1, 3, and 5 were shown in Figure 1. For the 1 cycle, numerous small dots of CuO were found over the FTO substrate and appeared as seed attachment. When the SILAR cycle was increased up to 3 and 5 cycles, the CuO film showed better coverage over the FTO surface according to the change in morphology. It should be noted that the surface morphology could not be made smooth under any of these conditions because film crystallization could not be totally controlled. To gain insight of CuO film topology, the AFM image was observed to investigate the surface change (Figure 1(d-f)). The change of surfaces was found for different number of SILAR cycles. This might be due to different reaction to form CuO for repeating adsorption and reaction processes. For roughness analysis, average roughness (R_a) was measured as 9.517, 13.183 and 10.099 nm for SILAR cycles of 1, 3, and 5 cycles, respectively. However, the results showed insignificant change in roughness or surface morphology. The copper oxide film thickness was measured using mapping AFM mode, and it was calculated as 25.71, 47.35 and 66.52 nm for SILAR cycles of 1, 3, and 5, respectively.

To examine the chemical composition of the CuO films, EDS of the film with different cycles was detected as shown in Figure 2. The Cu element cannot be detected with 1 cycle which can be explained because too little CuO is formed, which agreed with the morphological image. To classify the structural type of CuO films, the diffraction peaks were carried out using XRD as shown in Figure 3. It was found that the peaks of FTO substrate and FTO/CuO films were not much difference. The indifferent observed XRD peaks from both of samples could be due to ultrathin CuO film formation. The unclear XRD peaks resulted that CuO films cannot be clearly interpreted. Thus, optical micrograph was investigated as shown in the inset figure of Figure 3. The micrograph showed that film color were difference between FTO and FTO/CuO films. Dark-brown was and white-blue

were observed for the FTO and FTO/CuO, respectively. Therefore, it could be assumed that CuO films were formed according to the dark-brown in case of FTO/CuO films.

Optical transmission of the film was measured using UV-Vis-NIR as shown in Figure 4(a). The average transmission in the visible region was calculated as 98.07%, 97.02%, and 93.34% for 1, 3, and 5 cycles, respectively. In addition, the optical band gap energy (E_g) can be estimated from the transmission for direct band gap materials according to the relation [31]:

$$(\alpha h\nu)^2 = A(h\nu - E_g) \tag{1}$$

From the relation, the plot of $(\alpha h\nu)^2$ versus $h\nu$ is shown in Figure 4(b). The linear part was fitted to obtain E_g with a value of 1.94, 1.93, and 1.91 eV for 1, 3, and 5 cycles, respectively.

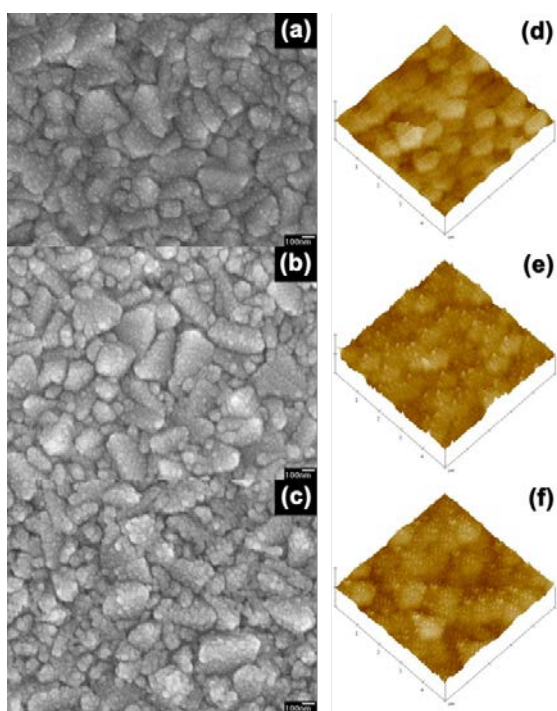


Figure 1. SEM images and AFM images of CuO film prepared on FTO substrate with different number of cycles: (a,d) 1, (b,e) 3, and (c,f) 5.

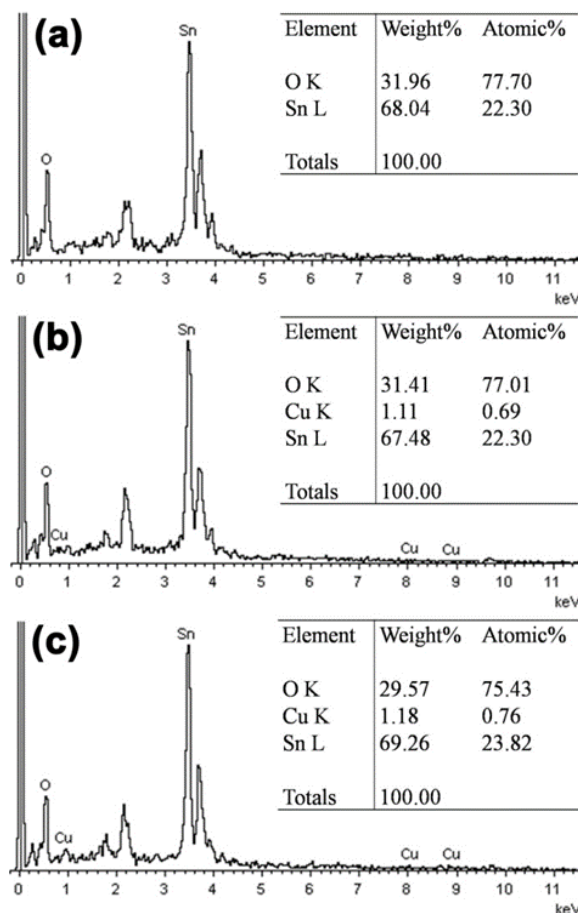


Figure 2. Chemical elements of CuO films prepared on FTO substrate with different number of cycles: (a) 1, (b) 3, and (c) 5.

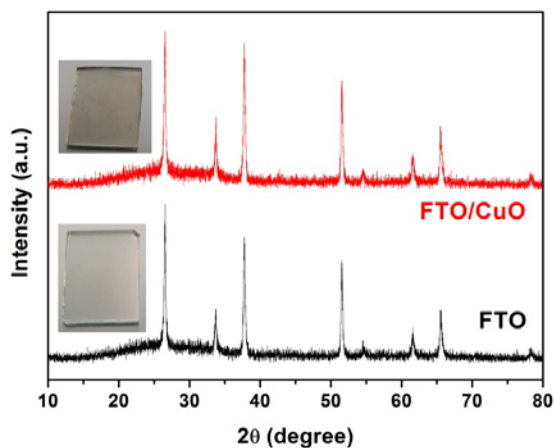


Figure 3. XRD patterns of FTO substrate and FTO/CuO films.

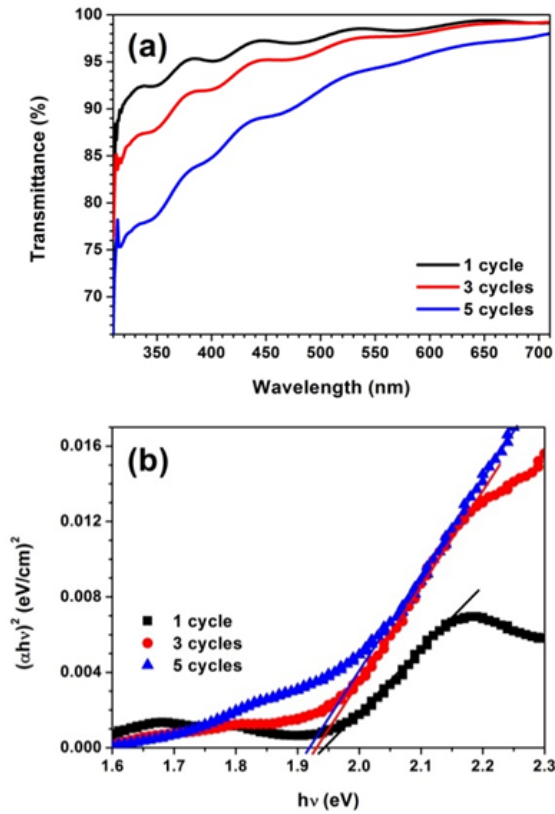


Figure 4. (a) Optical transmittance; and (b) optical band gap energy of CuO films prepared on FTO substrate for different cycles.

The CuO films were used as HTMs for p-i-n perovskite solar cells, and their performance was measured. Figure 5 shows the current density (J) versus the voltage (V) of the measured photovoltaic performance of the PSC fabricated using the CuO films. It was found that J_{sc} slightly increased with increasing cycles. The increase in J_{sc} indicates an improvement of charge collection for large cycles. The V_{oc} increased and reached a maximum with 3 SILAR processed cycles.

From the J-V curve, photovoltaic parameters were calculated and listed in Table 1. J_{sc} slightly increased correlating to the SILAR cycles, while the FF decreased. This effect might be described according to the relation:

$$FF = \frac{J_{max}V_{max}}{J_{sc}V_{oc}} \quad (2)$$

Table 1. Photovoltaic parameters of DSSC fabricated with CuO films using different numbers of cycles.

Number of SILAR cycles	J_{sc} (mA/cm ²)	V_{oc} (V)	FF	PCE (%)
1	3.97	0.57	0.44	1.00
3	4.71	0.65	0.39	1.20
5	5.60	0.50	0.36	1.00

Where J_{max} and V_{max} are maximal J and maximal V , respectively. The decrease in FF might be caused by a small change rate of maximum power ($J_{max}V_{max}$) compared with the ideal power ($J_{sc}V_{oc}$). This behavior was caused by the decreased shunt resistance (R_{sh}) of 307.28, 281.66 and 152.44 Ω for 1, 3 and 5 cycles. In addition, an occurrence of V_{oc} decrement for 5 cycles could be attributed to higher recombination rate of generated electron due to interfacial defect between CuO films and perovskite films.

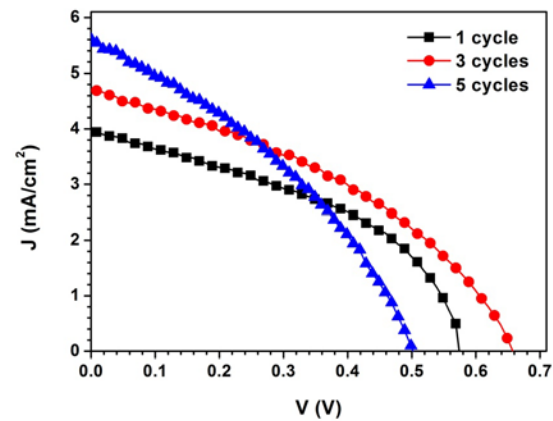


Figure 5. Current density versus voltage of p-i-n perovskite solar cell fabricated with CuO films.

To evaluate the benefits of the CuO films for p-i-n PSC application, the device fabricated with 3 SILAR processed CuO films was selected as the optimized device compared with PEDOT:PSS as shown in Figure 6. The photovoltaic parameters of the PEDOT:PSS based device for J_{sc} , V_{oc} , fill factor (FF), and PCE were 7.31 mA/cm², 0.75 V, 0.52, and 2.82%, respectively.

To investigate the behavior, morphology of $CH_3NH_3PbI_3$ perovskite films coated onto CuO films and PEDOT:PSS films were examined as shown in Figure 7. Unfortunately, perovskite films showed an incomplete formation when coated onto CuO films. The perovskite films revealed a combination of compact and porous zones, while better film formation was observed with only the compact zone when it was coated onto PEDOT:PSS.

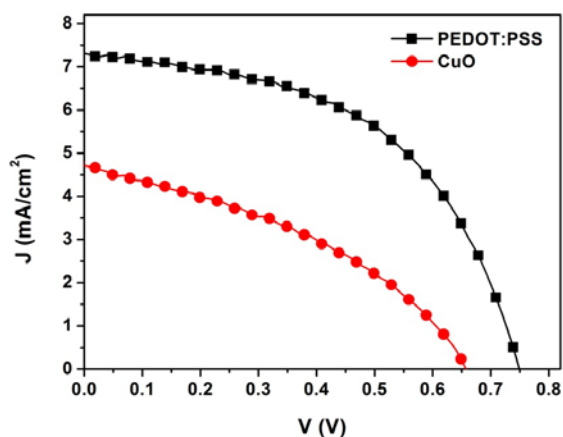


Figure 6. Current density - voltage characteristics under standard illumination of p-i-n perovskite solar cell fabricated with PEDOT:PSS and CuO films.

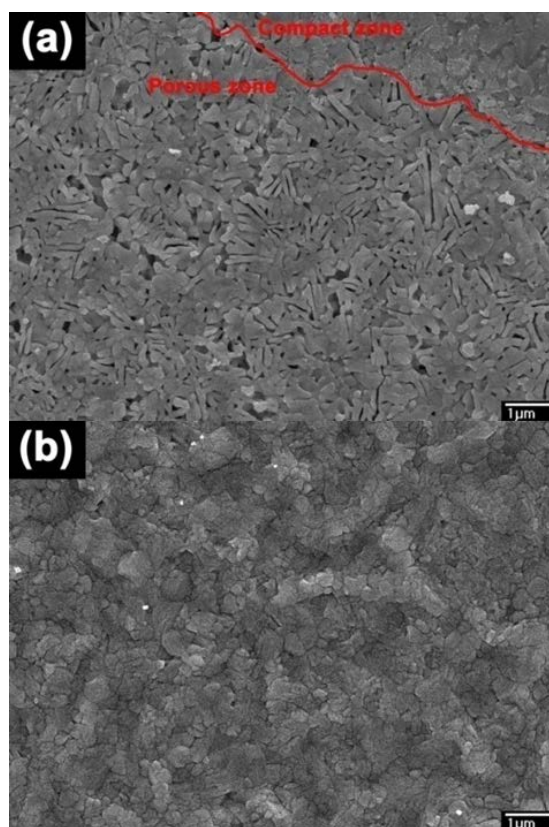


Figure 7. Morphology of perovskite films coated onto (a) FTO/CuO and (b) FTO/PEDOT:PSS.

Due to the porous perovskite film formation, direct contact between the HTMs and ETMs might have occurred. This defect causes a carrier loss in p-i-n PSCs due to a recombination effect [18], which can be interpreted from the higher current density under the dark condition for CuO films as shown in Figure 8. During electron-hole pair generation, electrons and holes are injected and transported in

ETMs and HTMs, respectively. They might be recombined due to direct HTM-ETM contact, leading to a carrier loss. Thus, this effect is believed to be a major factor in reducing p-i-n PSC performance.

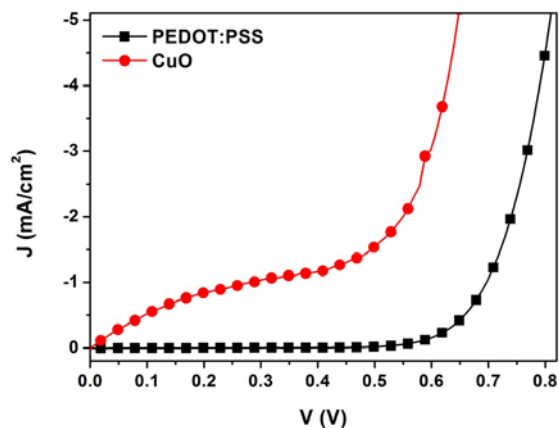


Figure 8. Current density - voltage characteristics measured under dark conditions.

4. Discussion

The seed attachment for 1 cycle can be explained by the lack of copper ions due to the low cycle preparation for CuO film formation [35]. However, the CuO films showed better coverage over the FTO substrate after number of cycles increased up to 3 and 5 cycles. This can be attributed to the filling of CuO at void positions to form a full coverage film after more cycles of SILAR process, which was agreed with the AFM results. Moreover, the results were correlated to the increasing appearance of Cu element. The XRD peaks of CuO cannot observe for prepared CuO films because the CuO might be very thin. The thin films could be reflected from high transmittance above 90% for all conditions. However, from the EDS results and the high annealing temperature, it could assume that the prepared films are CuO [30, 36-38].

For PSC application, the J_{sc} slightly increased with increasing cycles due to better coverage of the films over the substrate surface. Moreover, V_{oc} could be attributed an optimized value for 3 SILAR processed cycles. The decreased of FF was found opposite with increase of J_{sc} can be interpreted that maximum power is maintained or small changed. From the J-V curve, photovoltaic parameters were calculated and listed in Table 1. J_{sc} slightly increased correlating to the SILAR cycles, while the FF decreased. V_{oc} increased and reached maximum for 3 cycles, similar to PCE. Then, the PSC

fabricated with 3 cycles of CuO films was compared with PEDOT:PSS. The PSC fabricated with CuO films showed lower photovoltaic parameters than PEDOT:PSS because it revealed the porous perovskite film formation. Therefore, the results clearly suggested that the low performance in a p-i-n perovskite solar cell was due to porous perovskite film formation as seen from lost of the dark current. The formation with pore structures could reduce HTMs/PSSs/ETMs interfacial contact to form a p-i-n junction as the well known pinhole effect [16,39-40]. This work, however, demonstrated the ability of SILAR processed CuO films for applying as alternative HTMs in p-i-n PSC even through the films exhibited comparatively low performance. Note that for the p-i-n PSC performance improvement, the complete coverage of perovskite films on CuO films prepared using SILAR method should be further investigated. Different but efficient approaches could be considered such as control of film growth, doping with materials, surface treatment with solvent or vapor, and improved hydrophobic/hydrophilic property [41].

5. Conclusions

A demonstration of SILAR processed CuO films applied as a low cost hole-transporting material in a p-i-n perovskite solar cell was reported for the first time. The CuO films were prepared using SILAR method. The films had full coverage over substrate when the number of SILAR cycles increased; however, the open pores of perovskite films were still evident after deposition over the CuO films. This effect caused low levels of performance in p-i-n perovskite solar cell application compared with the commercial PEDOT:PSS hole-transporting material. However, the SILAR processed CuO films were shown to be suitable for use as alternative hole-transporting materials with a low fabrication cost for p-i-n perovskite solar cell application. To enhance device performance, the CuO films could be further investigated using various methods.

6. Acknowledgments

This work was supported by the Kasetsart University Research and Development Institute (KURDI), Kasetsart University, Bangkok, Thailand. The authors would like to acknowledge the Applied Physics Research Laboratory (APRL), Department

of Physics and Materials Science, Faculty of Science, Chiang Mai University, Chiangmai, Thailand for materials and device measurement; and Asst. Prof. Dr. Busba Tonthong, Kasetsart University and the KURDI for English editing advice and assistance.

References

- [1] A. Kojima, K. Teshima, Y. Shirai, and T. Miyasaka, "Organometal Halide Perovskites as Visible-Light Sensitizers for Photovoltaic Cells," *Journal of the American Chemical Society*, vol. 131, pp. 6050-6051, 2009.
- [2] N. Ahn, D.-Y. Son, I.-H. Jang, S. M. Kang, M. Choi, and N.-G. Park, "Highly Reproducible Perovskite Solar Cells with Average Efficiency of 18.3% and Best Efficiency of 19.7% Fabricated via Lewis Base Adduct of Lead(II) Iodide," *Journal of the American Chemical Society*, vol. 137, pp. 8696-8699, 2015.
- [3] K. Hwang, Y.-S. Jung, Y.-J. Heo, H. F. Scholes, S. E. Watkins, J. Subbiah, D. J. Jones, D.-Y. Kim, and D. Vak, "Toward Large Scale Roll-to-Roll Production of Fully Printed Perovskite Solar Cells," *Advanced Materials*, vol. 27, pp. 1241-1247, 2015.
- [4] N.-G. Park, "Perovskite solar cells: an emerging photovoltaic technology," *Materials Today*, vol. 18, 65-72, 2015.
- [5] M.-E. Ragoussi and T. Torres, "New generation solar cells: concepts, trends and perspectives," *Chemical Communications*, vol. 51, pp. 3957-3972, 2015.
- [6] S. Razza, F. Di Giacomo, F. Matteocci, L. Cina, A. L. Palma, S. Casaluci, P. Cameron, A. D'Epifanio, S. Licoccia, A. Reale, T. M. Brown, and A. Di Carlo, "Perovskite solar cells and large area modules (100 cm²) based on an air flow-assisted PbI₂ blade coating deposition process," *Journal of Power Sources*, vol. 277, pp. 286-291, 2015.
- [7] L. Etgar, P. Gao, Z. Xue, Q. Peng, A. K., Chandiran, B. Liu, M. K. Nazeeruddin, and M. Gratzel, "Mesoscopic CH₃NH₃PbI₃/TiO₂ Heterojunction Solar Cells," *Journal of the American Chemical Society*, vol. 134, pp. 17396-17399, 2012.
- [8] H.-S. Kim, C.-R. Lee, J.-H. Im, K.-B. Lee, T. Moehl, A. Marchioro, S.-J. Moon, R. Humphry-Baker, J.-H. Yum, J. E. Moser, M.

- Gratzel, and N.-G. Park, "Lead Iodide Perovskite Sensitized All-Solid-State Submicron Thin Film Mesoscopic Solar Cell with Efficiency Exceeding 9%," *Scientific Reports*, vol. 2, pp. 591, 2012.
- [9] M. Liu, M. B. Johnston, and H. J. Snaith, "Efficient planar heterojunction perovskite solar cells by vapour deposition," *Nature*, vol. 501, pp. 395-398, 2013.
- [10] D. Liu and T. L. Kelly, "Perovskite solar cells with a planar heterojunction structure prepared using room-temperature solution processing techniques," *Nature Photonics*, vol. 8, pp. 133-138, 2014.
- [11] J. Burschka, N. Pellet, S.-J. Moon, R. Humphry-Baker, P. Gao, M. K. Nazeeruddin, and M. Gratzel, "Sequential deposition as a route to high-performance perovskite-sensitized solar cells," *Nature*, vol. 499, pp. 316-319, 2013.
- [12] S. Luo and W. A. Daoud, "Recent progress in organic-inorganic halide perovskite solar cells: mechanisms and material design," *Journal of Materials Chemistry A*, vol. 3, pp. 8992-9010, 2015.
- [13] J. H. Heo, H. J. Han, D. Kim, T. K. Ahn, and S. H. Im, "Hysteresis-less inverted CH₃NH₃PbI₃ planar perovskite hybrid solar cells with 18.1% power conversion efficiency," *Energy and Environmental Science*, vol. 8, pp. 1602-1608, 2015.
- [14] Z. Zhou, S. Pang, Z. Liu, H. Xu, and G. Cui, "Interface engineering for high-performance perovskite hybrid solar cells," *Journal of Materials Chemistry A*, vol. 3, pp. 19205-19217, 2015.
- [15] C.-Y. Chang, C.-Y. Chu, Y.-C. Huang, C.-W. Huang, S.-Y. Chang, C.-A. Chen, C.-Y. Chao, and W.-F. Su, "Tuning Perovskite Morphology by Polymer Additive for High Efficiency Solar Cell," *ACS Applied Materials and Interfaces*, vol. 7, pp. 4955-4961, 2015.
- [16] S. Bag and M. F. Durstock, "Large Perovskite Grain Growth in Low-Temperature Solution-Processed Planar p-i-n Solar Cells by Sodium Addition," *ACS Applied Materials and Interfaces*, vol. 8, pp. 5053-5057, 2016.
- [17] R. Betancur, D. Ramirez, J. F. Montoya, and F. Jaramillo, "A calorimetric approach to reach high performance perovskite solar cells," *Solar Energy Materials and Solar Cells*, vol. 146, pp. 44-50, 2016.
- [18] T. Du, N. Wang, H. Chen, H. Lin, and H. He, "Comparative Study of Vapor- and Solution-Crystallized Perovskite for Planar Heterojunction Solar Cells," *ACS Applied Materials and Interfaces*, vol. 7, pp. 3382-3388, 2015.
- [19] Y. Li, J. K. Cooper, R. Buonsanti, C. Giannini, Y. Liu, F. M. Toma, and I. D. Sharp, "Fabrication of Planar Heterojunction Perovskite Solar Cells by Controlled Low-Pressure Vapor Annealing," *The Journal of Physical Chemistry Letters*, vol. 6, pp. 493-499, 2015.
- [20] H. Tsai, W. Nie, P. Cheruku, N. H. Mack, P. Xu, G. Gupta, A. D. Mohite, and H.-L. Wang, "Optimizing Composition and Morphology for Large-Grain Perovskite Solar Cells via Chemical Control," *Chemistry of Materials*, vol. 27, pp. 5570-5576, 2015.
- [21] A. S. Subbiah, A. Halder, S. Ghosh, N. Mahuli, G. Hodes, and S. K. Sarkar, "Inorganic hole conducting layers for perovskite-based solar cells," *Journal of Physical Chemistry Letters*, vol. 5, pp. 1748-1753, 2014.
- [22] M. Habibi, F. Zabihi, M. R. Ahmadian-Yazdi, and M. Eslamian, "Progress in emerging solution-processed thin film solar cells – Part II: Perovskite solar cells," *Renewable and Sustainable Energy Reviews*, vol. 62, pp. 1012-1031, 2016.
- [23] H. Rao, S. Ye, W. Sun, W. Yan, Y. Li, H. Peng, Z. Liu, Z. Bian, Y. Li, and C. Huang, "A 19.0% efficiency achieved in CuOx-based inverted CH₃NH₃PbI₃-xCl_x solar cells by an effective Cl doping method," *Nano Energy*, vol. 27, pp. 51-57, 2016.
- [24] Z.-K. Yu, W.-F. Fu, W.-Q. Liu, Z.-Q. Zhang, Y.-J. Liu, J.-L. Yan, T. Ye, W.-T. Yang, H.-Y. Li, and H.-Z. Chen, "Solution-processed CuOx as an efficient hole-extraction layer for inverted planar heterojunction perovskite solar cells," *Chinese Chemical Letters*, vol. 28, pp. 13-18, 2017.
- [25] C. Zuo, and L. Ding, "Solution-Processed Cu₂O and CuO as Hole Transport Materials for Efficient Perovskite Solar Cells," *Small*, vol. 11, pp. 5528-5532, 2015.
- [26] Y. Guo, H. Lei, L. Xiong, B. Li, Z. Chen, J. Wen, G. Yang, G. Li, and G. Fang, "Single

- phase, high hole mobility Cu₂O films as an efficient and robust hole transporting layer for organic solar cells,” *Journal of Materials Chemistry A*, vol. 5, pp. 11055-11062, 2017.
- [27] Z. H. Bakr, Q. Wali, A. Fakharuddin, L. Schmidt-Mende, T. M. Brown and R. Jose, “Advances in hole transport materials engineering for stable and efficient perovskite solar cells,” *Nano Energy*, vol. 34, pp. 271-305, 2017.
- [28] L. Liu, Q. Xi, G. Gao, W. Yang, H. Zhou, Y. Zhao, C. Wu, L. Wang, and J. Xu, “Cu₂O particles mediated growth of perovskite for high efficient hole-transporting-layer free solar cells in ambient conditions,” *Solar Energy Materials and Solar Cells*, vol. 157, pp. 937-942, 2016.
- [29] L. Wang, R. Zhang, T. Zhou, Z. Lou, J. Deng, and T. Zhang, “P-type octahedral Cu₂O particles with exposed {111} facets and superior CO sensing properties,” *Sensors and Actuators B: Chemical*, vol. 239, pp. 211-217, 2017.
- [30] S. Chatterjee, S. K. Saha, and A. J. Pal, “Formation of all-oxide solar cells in atmospheric condition based on Cu₂O thin-films grown through SILAR technique,” *Solar Energy Materials and Solar Cells*, vol. 147, pp. 17-26, 2016.
- [31] S. Chatterjee, and A. J. Pal, “Introducing Cu₂O Thin Films as a Hole-Transport Layer in Efficient Planar Perovskite Solar Cell Structures,” *The Journal of Physical Chemistry C*, vol. 120, pp. 1428-1437, 2016.
- [32] W. Yu, F. Li, H. Wang, E. Alarousu, Y. Chen, B. Lin, L. Wang, M. N. Hedhili, Y. Li, K. Wu, X. Wang, O. F. Mohammed, and T. Wu, “Ultrathin Cu₂O as an efficient inorganic hole transporting material for perovskite solar cells,” *Nanoscale*, vol. 8, pp. 6173-6179, 2016.
- [33] A. S. Patil, G. M. Lohar, and V. J. Fulari, “Structural, morphological, optical and photoelectrochemical cell properties of copper oxide using modified SILAR method,” *Journal of Materials Science: Materials in Electronics*, vol. 27, pp. 9550-9557, 2016.
- [34] S. Sutthana, K. Hongsith, P. Ruankham, D. Wongratanaphisan, A. Gardchareon, S. Phadungdhithidhada, D. Boonyawan, P. Kumnorkaew, A. Tuantranont, and S. Choopun, “Interface modification of CH₃NH₃PbI₃/PCBM by pre-heat treatment for efficiency enhancement of perovskite solar cells,” *Current Applied Physics*, vol. 17, pp. 488-494, 2017.
- [35] A. Banerjee, D. Prusty, M. Dutta, A. K. Bhowmick and T. Laha, “Effect of Cu₂O thin film on Cu–Sn alloy coated steel surface in promoting interfacial adhesion with rubber,” *Journal of Adhesion Science and Technology*, vol. 31, pp. 1163-1180, 2017.
- [36] L.-C. Chen, C.-C. Chen, K.-C. Liang, S. H. Chang, Z.-L. Tseng, S.-C. Yeh, C.-T. Chen, W.-T. Wu, and C.-G. Wu, “Nano-structured CuO-Cu₂O Complex Thin Film for Application in CH₃NH₃PbI₃ Perovskite Solar Cells,” *Nanoscale Research Letters*, vol. 11, pp. 402, 2016.
- [37] A. S. Patil, M. D. Patil, G. M. Lohar, S. T. Jadhav, and V. J. Fulari, “Supercapacitive properties of CuO thin films using modified SILAR method,” *Ionics*, vol. 23, pp. 1259-1266, 2017.
- [38] S. Visalakshi, R. Kannan, S. Valanarasu, A. Kathalingam, and S. Rajashabala, “Studies on optical and electrical properties of SILAR-deposited CuO thin films,” *Materials Research Innovations*, vol. 21, pp. 146-151, 2017.
- [39] G. Adam, M. Kaltenbrunner, E. D. Głowacki, D. H. Apaydin, M. S. White, H. Heilbrunner, S. Tombe, P. Stadler, B. Ernecker, C. W. Klampfl, N. S. Sariciftci, and M. C. Scharber, “Solution processed perovskite solar cells using highly conductive PEDOT:PSS interfacial layer,” *Solar Energy Materials and Solar Cells*, vol. 157, pp. 318-325, 2016.
- [40] W. Qiu, T. Merckx, M. Jaysankar, C. Masse de la Huerta, L. Rakocevic, W. Zhang, U. W. Paetzold, R. Gehlhaar, L. Froyen, J. Poortmans, D. Cheyns, H. J. Snaith, and P. Heremans, “Pinhole-free perovskite films for efficient solar modules,” *Energy and Environmental Science*, vol. 9, 484-489, 2016.
- [41] C. Bi, Q. Wang, Y. Shao, Y. Yuan, Z. Xiao, and J. Huang, “Non-wetting surface-driven high-aspect-ratio crystalline grain growth for efficient hybrid perovskite solar cells,” *Nature Communications*, vol. 6, pp. 1-7 2015.